DEGRADATION OF AMINO ACIDS BY MeV NITROGEN IONS

C.A.P. DA COSTA†[1]
Physics Departament, Pontifical Catholic University of Rio de Janeiro (PUC-Rio)
Rio de Janeiro, Brazil
Email: cintia-apc@hotmail.com

E. F. DA SILVEIRA
Physics Departament, Pontifical Catholic University of Rio de Janeiro (PUC-Rio)
Rio de Janeiro, Brazil

Abstract

The occurrence of amino acids in meteorites and comets raises questions about how they have been formed in cosmic environments, as well as how long they can survive in outer space; radioresistance is essential information to predict half-lives and make advances on the origins of life studies. Furthermore, amino acid radiolysis is of Medical Physics interest. The main objective of the current work is to analyze, via infrared spectrometry, how destruction cross section of pure valine exposed to energetic ion radiation depends on projectile's energy and charge. Apparent destruction cross sections (σ_d^{ap}) and sputtering yields (Y_0) for this amino acid irradiated by MeV N^{q+} ions were measured. Degradation of the amino acid valine by nitrogen beams under different conditions such as several charge states (N^{q+}, q = 1, 2 and 3) and energies (1.5 and 6.0 MeV) is analyzed. From experimental data of this and previous measurements it is concluded that: i) an approximately linear dependence between the apparent destruction cross section and the electronic stopping power (S_e) is proposed for MeV projectiles, and for samples at room temperature; and ii) σ_d^{ap} results concerning multi-charged nitrogen ion beams are discussed. As astrophysical application, cosmic ray half-lives for valine are estimated to be about 10 million years in the interstellar medium; concerning hadronterapy, the question is whether to decrease the initial projectile charge state may be useful.

1. INTRODUCTION

Degradation of organic materials exposed to ionizing radiation has an enormous relevance in areas such as Medical Physics (Radiotherapy, production and application of radioisotopes), Radiological Security of nuclear plants and large accelerator laboratories, manned missions in the Solar System, and Astrochemistry (evolution of molecular species in the Universe). Although main lines concerning the interaction of energetic electrons, ions and photons with organic matter are under research since long time, specific information is still necessary.

The focus of this work is in one of these specific systems: MeV ion beams impinging on prebiotic molecules. The scenario can be constrained as well, represented by the following question: what is the degradation rate of some common amino acids exposed to Solar Wind or to Galactic Cosmic Rays?

Indeed, the main amino acids (vital for living beings) and some other complex organic molecules (COMs) have been found in meteorites such as Murray, Murchison, Nogoya and Mokoia [1–3]. In particular, glycine (Gly) has been detected indirectly by the Stardust probe in dust traces of the comet 81P/Wild 2 [4], and directly, in considerable large quantities, in jets of the comet 67P/Churyumov-Gerasimenko by the Rosetta mission [5]. The detection of valine (Val) molecules has not been confirmed yet, but since these materials are present in meteorites, they might exist elsewhere in the outer space too. Moreover, if larger molecules such as PAHs (Polycyclic Aromatic Hydrocarbons) exist throughout diverse astronomical environments [6], the detection of amino acids in the interstellar medium is expected.

In space, those materials are exposed to several kinds of radiation. From an abiotic origin of life point of view, relevant questions appear, such as: does space radiation have a role in the synthesis of COMs? Is cosmic organic matter responsible for the existence of life as we know? Considering astronomical low temperature and pressure conditions, the "Chemistry of life" would not be able to occur spontaneously in these environments: some kind of catalyzer should be necessary. The specific places where those materials occur are also very important. For instance, molecules within asteroids or comets are shielded from short-range radiation, being available then to be delivered in hospitable zones where more complex organic chemistry may happen until the

---

†*Present Address: Research Center for Ions, Materials And Photonic (CIMAP - GANIL), CAEN – FRANCE*

development of life. Nevertheless, for this same example, such molecules could be exposed to radionuclide decay inside the considered celestial bodies [7–9]. Furthermore, the low albedo (dark gray) of these astrophysical specimens is probably related to the graphitization / carbonization of carbon-content material existing on their surfaces: ionizing radiation turns the condensed original material (e.g., CH_4, $HCONH_2$, CO_2) into carbon enriched compounds as polymeric C_nH_2 chains or tholins [10, 11]. It is significant, then, to explore how amino acids are affected by energetic ions, similar to those constituents of cosmic radiation, in order to estimate their radioresistance, and respective half-lives in astronomical environments.

In hadrontherapy, it is well known that the beam energy is crucial for irradiations: the highest stopping power must occur in the tumor region [12]. Because this region is generally deep, the ion beam is in the so called equilibrium charge state and does not depend on the external beam charge state. However, the point here is that molecular destruction rate of the patient's skin is significantly reduced if the initial charge state of the ion beam is decreased. The relevant question becomes how deep MeV heavy ion beams take to reach their equilibrium charge. The measurement of valine (as a typical biological material) destruction cross section as a function of the nitrogen beam charge state is a contribution in this direction. The employed nitrogen beam energy were about 1 MeV (two orders of magnitude lower than beams used in hadronterapy), and the valine samples thickness were around 40 nm.

The goals of the present work are:

— Determine cross sections of valine irradiated by nitrogen MeV ions;
— Confirm whether valine cross section depends linearly on the beam stopping power, and discuss the projectile charge effects on degradation;
— Study the projectile-material interaction, and the physical processes behind experimental results;
— Estimate relevant parameters, such as degradation rates, that might be useful for other research areas.

Sections 2 and 3 describe the experimental techniques and results of the current research, respectively. In Section 4 results are discussed, as well as possible applications. The main conclusions are presented in Section 5.

2. EXPERIMENTAL SETUP

Valine dissociation by nitrogen MeV ions was monitored at the PUC-Rio Van de Graaff Laboratory. Ion beams of 1.5 MeV N^+, N^{2+}, N^{3+} and 6.0 MeV N^{2+} were produced by a Van de Graaff accelerator and bombarded, perpendicularly, the targets at room temperature. Distinct charged projectiles were obtained by accelerating N^+ projectiles, selecting the desired kinetic energy by a 90° analysing magnet, introducing the beam in a gas stripper to create N^{q+} ions and filtering a given projectile charge state by 15° magnet. The pressure in the stripper was varied in order to maximize the beam intensity for that charge state.

The residual gas pressure in the vacuum chamber was around 10^{-7} mbar; for a detailed description, see Pilling et al. (2013) [13] and da Costa et al. (2021) [14]. Evolution of sample destruction was monitored by a JASCO FTIR-4100 infrared spectrometer. The Fourier Transform Infrared spectroscopy (FTIR) spectra were acquired over the 3500–700 cm^{-1} range, in transmission mode; spectral resolution of 2.0 cm^{-1} and averaging 70 scans.

Thin films, ~ 25 – 65 nm, of valine (Sigma Aldrich, 99% purity) were deposited in vacuum onto ZnSe substrates. Valine density was taken as 1.32 g cm^{-3} [15].

3. RESULTS

3.1. Beam charge state (N^{q+})

Five L-valine samples, ~ 25 nm thick, were bombarded by 1.5 MeV N^+, N^+, N^{2+}, N^{3+} and 6.0 MeV N^{2+}. Different charge states were obtained by a selector magnet, as described in section 2. For each beam the evolutions of the IR bands 3190-2430, 1602-1579 (1507), and 1337-1320 (1330) cm^{-1} were followed and their respective normalized integrated absorbance is displayed on Figures 1 (a) – (c) and 2; lines are fittings and the obtained destruction cross sections are presented in the same color code.

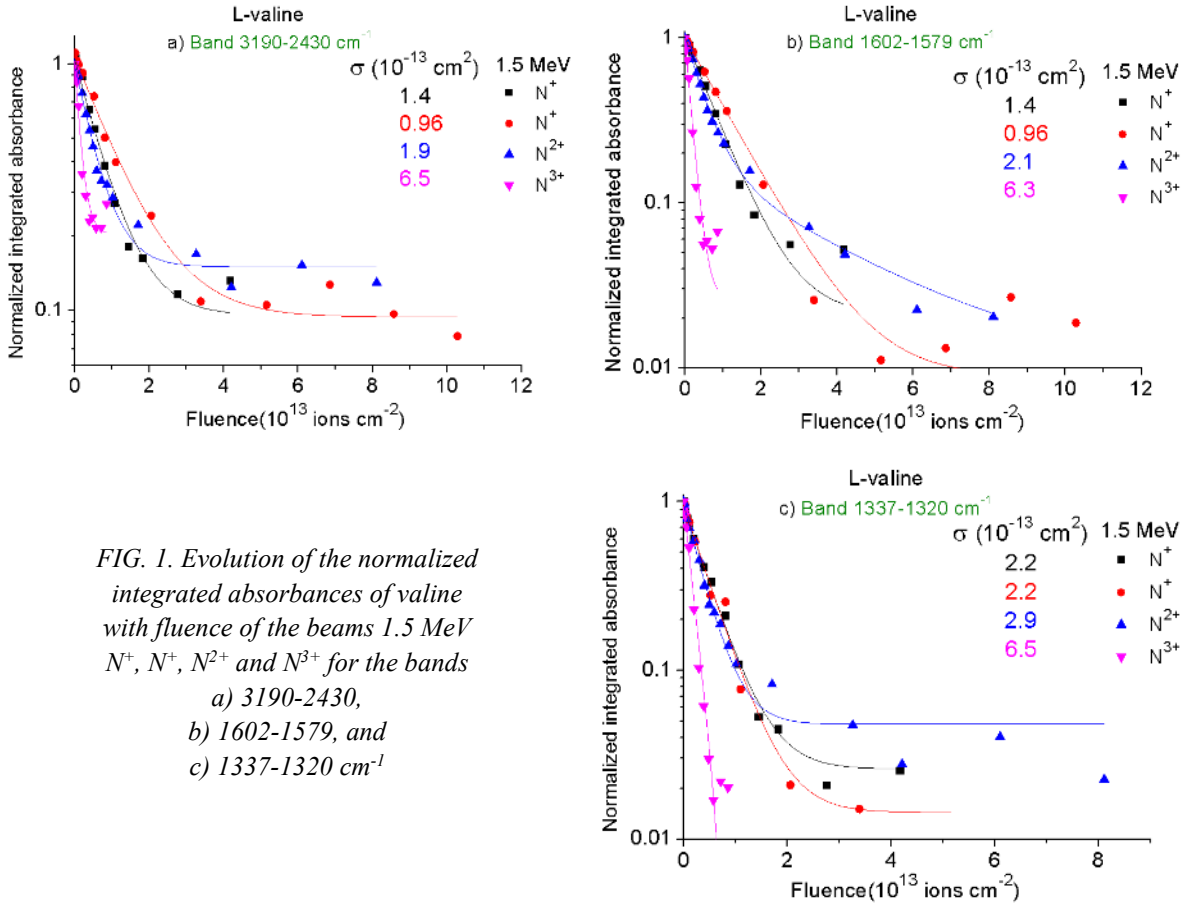

FIG. 1. Evolution of the normalized integrated absorbances of valine with fluence of the beams 1.5 MeV N^+, N^+, N^{2+} and N^{3+} for the bands a) 3190-2430, b) 1602-1579, and c) 1337-1320 cm^{-1}

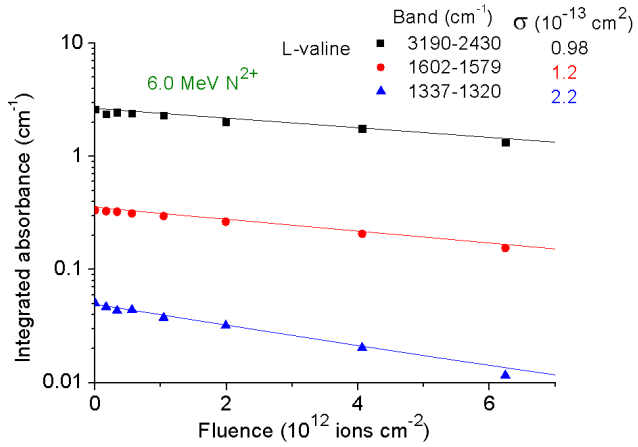

FIG. 2. Evolution of the normalized integrated absorbances of valine with fluence of the beam 6.0 MeV N^{2+} for the bands 3190-2430, 1602-1579, and 1337-1320 cm^{-1}.

Table 1 summarizes the fitting parameters. The strong decrease of the integrated absorbance of the 1337-1320 band may be attributed to sputtering.

3.2. Dependence on Sample thickness

Three L-valine samples with thicknesses 27.5, 44.2 and 64.9 nm were irradiated by ions of 1.5 MeV N^+. In figures 3 (a) – (c), the evolutions of these three samples in function of beam fluence is presented for the 3190-2430, 1602-1579 and 1337-1320 cm^{-1} bands. Table 2 summarizes the fitting parameters.

TABLE 1. Parameters obtained from the fitting of the integrated absorbances decay with the function $S(F) = S_0 \exp(-\sigma F) + S_\infty$. Data from valine irradiated by 1.5 and 6.0 MeV multi-charged nitrogen beams.

Sample	Beam	Band (cm^{-1})	S_0 (cm^{-1})	σ (10^{-16} cm^2)	S_∞ (cm^{-1})
L-Val	1.5 MeV N^+	3190-2430	0.95	1400	0.096
		1602-1579	0.99	1400	0.01
		1337-1320	0.91	2200	0.026
	1.5 MeV N^+	3190-2430	0.97	960	0.094
		1602-1579	0.99	960	0.01
		1337-1320	0.94	2200	0.014
	1.5 MeV N^{2+}	3190-2430	0.85	1900	0.15
		1602-1579	0.83	2100	0.17
		1337-1320	0.92	2900	0.048
	1.5 MeV N^{3+}	3190-2430	0.82	6500	0.20
		1602-1579	0.96	6300	0.03
		1337-1320	0.99	6500	-
	6.0 MeV N^{2+}	3190-2430	2.65	980	-
		1602-1579	0.35	1200	-
		1337-1320	0.048	2200	-

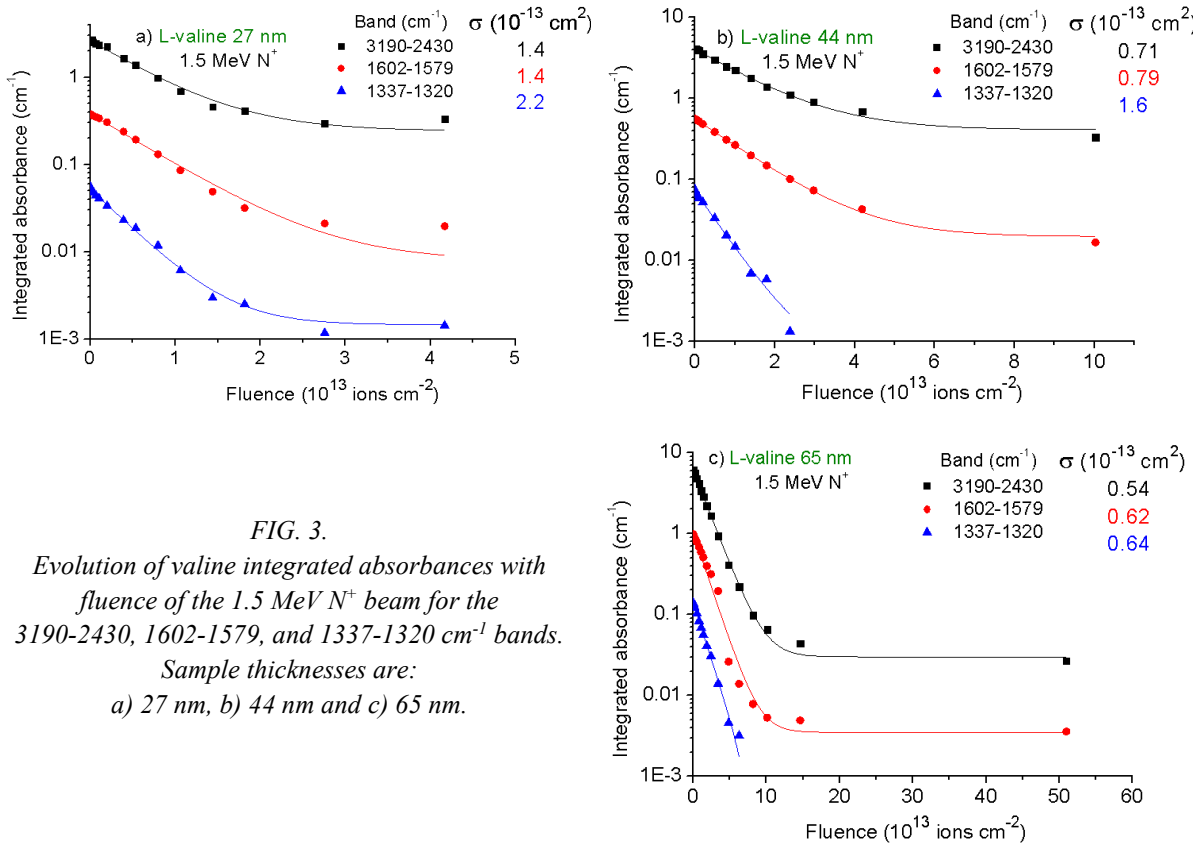

FIG. 3.
Evolution of valine integrated absorbances with fluence of the 1.5 MeV N^+ beam for the 3190-2430, 1602-1579, and 1337-1320 cm^{-1} bands. Sample thicknesses are: a) 27 nm, b) 44 nm and c) 65 nm.

4. DISCUSSION

4.1. Multi-charged beams

Sputtering and radiolysis are sensitive to projectile charge; yields of both processes are expected to be proportional to $S_e^n \sim (q^2)^n$. For icy samples, n = 2 have been reported for sputtering (e.g. Seperuelo-Duarte et al.

(2010) [16]) and n = 1 to 1.5 for radiolysis. Experiments with multi-charged beams were carried out to verify the sensitivity of amino acid's damage to the projectile charge. The measurements involved experimental challenges such as production, selection, transport and monitoring of multi-charged beams. The high sensitivity of stopping powers on projectile charge state indicates that further experiments are necessary to be compared with the current results.

1.5 MeV N^+ ions were produced by the Van de Graaff accelerator and selected by the 90º analyzing magnet. The residual gas inside the 4.9 m long canalization between this magnet and the switching one was raised to around 10^{-4} mbar for enhancing ion beam charge exchange. At 1.5 MeV energy, projectiles have v = 4.5 x 10^3 km/s, and the equilibrium charge state distribution is N^{3+} (48%), N^{2+} (27%), N^{4+} (19%), N^{1+} (4%) and N^{5+} (2%) [17]. The average equilibrium charge state is, therefore, q_{eq} = 2.9; CasP (Convolution approximation for swift Particles) prediction is 2.1 [18].

After, crossing a 10^{-6} mbar residual gas, the N^+, N^{2+} and N^{3+} charge state beams were selected by an adequate magnetic field at the switching magnet and transported via a ~5 m canalization up to the UHV section (at <10^{-7} mbar), see Pilling et al. (2013) [13]. Fluence was calculated assuming that no charge exchange has occurred between the switching magnet and the Faraday cup inside the FTIR chamber.

Valine samples, ~ 25 nm thick, were irradiated by 1.5 MeV N^{q+} with charge states q = 1, 2 and 3. Samples must be thin enough, not only to be traversed by the beam, but also for allowing it (ideally) to exit without reaching the equilibrium charge. On the other hand, 15-20 nm is typically the thinnest initial thickness range compatible to the infrared spectrometer sensibility, considering that the decrease of absorbances with beam fluence should be strong enough for permitting the σ_d^{ap} measurement.

For each experiment, the average σ_d^{ap} was calculated from three bands analyzed in Fig. 1 – see Table 3. Clearly, the higher the projectile charge, the greater the apparent destruction cross section measured.

TABLE 2. Parameters obtained from the fitting of the integrated absorbances decay with the function $S(F) = S_0 \exp(-\sigma F) + S_\infty$. Data from valine with distinct thicknesses irradiated by 1.5 MeV N^+.

Thickness (nm)	Band (cm^{-1})	S_0 (cm^{-1})	σ (10^{-16} cm^2)	S_∞ (cm^{-1})
27	3190-2430	2.40	1400	0.24
	1602-1579	0.37	1400	0.008
	1337-1320	0.051	2200	0.0014
44	3190-2430	3.66	710	0.41
	1602-1579	0.54	790	0.020
	1337-1320	0.071	1600	0.001
65	3190-2430	6.07	540	0.03
	1602-1579	1.02	620	0.0035
	1337-1320	0.14	640	-

TABLE 3. Apparent destruction cross sections of 1.5 MeV N^{q+} on valine samples.

Charge state	σ_d^{ap} (10^{-13} cm^2)			
	Analyzed band (cm^{-1})			Average
	3190-2430	1602-1579	1337-1320	
1+	1.4	1.4	2.2	1.7 ± 0.5
1+	0.96	0.96	2.2	1.4 ± 0.8
2+	1.9	2.1	2.9	2.3 ± 0.6
3+	6.5	6.3	6.5	6.4 ± 0.1

Under the perspective of a radiolysis analysis, Figure 4 (a) shows the average σ_d^{ap} dependence on q^2. Then, as $\sigma^{3+}/\sigma^+ = 4.1$ and $\sigma^{2+} / \sigma^+ = 1.5$, the average beam charge state ratios inside the samples are ~ 2.0 and 1.2 (instead of 3 and 2) for N^{3+}/N^+ and N^{2+}/N^+, respectively. By combining Eq. (1) with Joy-Luo-Bethe-Bloch's formula [19, 20], the average cross section for a projectile with charge z and velocity v can be estimated as

$$\sigma_d^{ap}(q,v) = a\, S_e(q,v) = a\, S_e^{e^-}(v)\, q^2 = \sigma_d^{ap}(e^-,v)\, q^2, \qquad (1)$$

where $S_e^{e-}(v)$ and σ_d^{ap} (e^-,v) are the stopping power and the destruction cross section for electron projectiles with the same velocity v, respectively. For a dominant radiolysis damage, a proportionality is expected in a graph σ_d^{ap} (q,v) versus q^2, in which σ_d^{ap} (e^-,v) is the angular coefficient, if no charge exchange occurs inside the sample. 1.5 MeV N ions and 59 eV electrons have the same velocity: v = 4.5 x 10^3 km/s. For valine, a = 1.0 x 10^{-20} cm^3 keV^{-1}; 59 eV electrons have S_e^{e-} ~ 8 eV Å $^{-1}$ = 8 x 10^5 keV cm^{-1}; the Joy-Luo formula with k = 0.6 provides σ_d^{ap} (e^-,v) = 0.8 x 10^{-14} cm^2. This result is to be compared with the angular coefficient of experimental data (dotted line in Fig. 4), which is roughly 6 x 10^{-14} cm^2 (per square charge state). CasP results, imposing no charge exchange inside the sample, agree with the cross section ~ 1 x 10^{-14} cm^2 for q = 1; on the other hand, it predicts an angular coefficient of 0.4 x10^{-14} cm^2, twice lower than Joy-Luo result, but much lower than the experimental value. A discussion on equilibrium charge state follows.

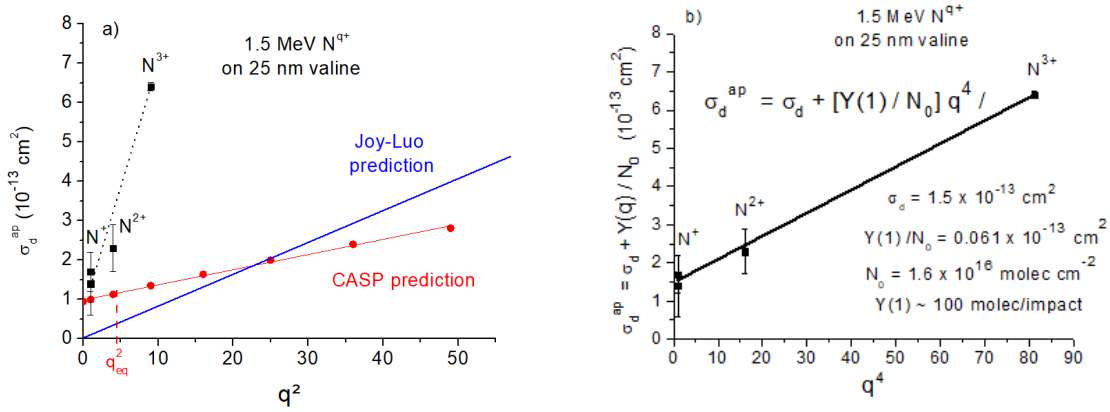

FIG. 4. σ_d^{ap} dependence on initial beam charge state; 1.5 MeV N^{q+} beam impinging on valine 25 nm thick: q = 1, 1, 2 and 3. a) Linear fitting of data (dotted line) has a slope = 6 x 10^{-14} cm^2 per square charge state. The Bethe-Bloch's function prediction is valid if no charge exchange occurs. When a neutral 1.5 MeV N projectile enters in a solid target, it looses one or more electrons; therefore, in average, collisions in the bulk occur with $q \neq 0$ and σ_d^{ap} cannot be zero. In contrast, CasP predicts this stopping power (and σ_d^{ap}) correctly [18]. b) Assuming only sputtering ($\sigma_d^{ap} \sim q^4$).

Inside a solid, a projectile with initial charge state q captures and loses electrons until its charge state reaches an average equilibrium value, q_{eq} [21-23]. Equation (2) is the expression for this equilibrium charge according to Bohr's adiabatic criterion, where the projectile electrons with orbital velocities smaller than the projectile translation velocity are removed during the collision cascade with target atoms [24]; Z_p being the projectile atomic number, v its velocity and v_B the Bohr's velocity.

$$q_{eq} = Z_p \left[1 - exp\left(\frac{-125\, v}{137\, v_B Z_p^{2/3}}\right)\right] \qquad (2)$$

Figure 5 presents the predicted equilibrium charge, acording to Eq. (2), in function of nitrogen projectile velocities. A nitrogen projectile with 1.5 MeV of kinetic energy has the velocity v = 0.45 cm ns^{-1} and a predicted equilibrium charge of q_{eq} ~ 2.8. Other q_{eq} expressions from more refined models, as those of Montenegro et al. (1982) [25], Heckman et al. (1963) [26] and Grande and Schiwietz (1998) [18] give similar results within 10% error [22]; for simplicity, Eq. (2) is the approach taken.

The projectile charge evolves asymptotically inside the material from q (the incident projectile charge) to reach q_{eq} (the final projectile mean charge). Between q and q_{eq} the charge has a transient or average value that is a function of the covered distance by the projectile, $q_{av}(s)$. Bohr has proposed that the projectile charge state inside a material should be written as Eq. (3) [27]:

$$q_{av}(s) = q_{eq} + (q - q_{eq}) exp\left(-\frac{s}{\lambda_q}\right) \qquad (3)$$

with s being the projectile's covered distance along the track, and λ_q the characteristic relaxation length of the solid. Based on Eq. (3), Fig. 6 presents $q_{av}(s)$ for 1.5 MeV N^{q+} ion beams with initial charge states q = 1 and q = 3 impinging on a solid of icy water. Both beams reach the equilibrium charge around s = 4 nm inside the sample. Although the λ_q value for valine is not known, the rougthly linear relationship between σ_d^{ap} and q^2 in Fig. 4 suggests that λ_q is is much higher than 4 nm and comparable to the sample thickness.

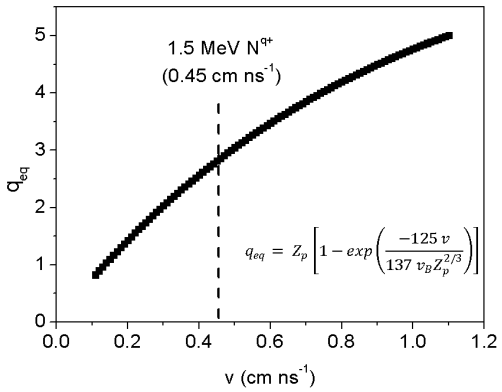

FIG. 5. Equilibrium charge state in function of nitrogen ions velocities. The vertical dash line indicates the velocity of the beam used in this data set.

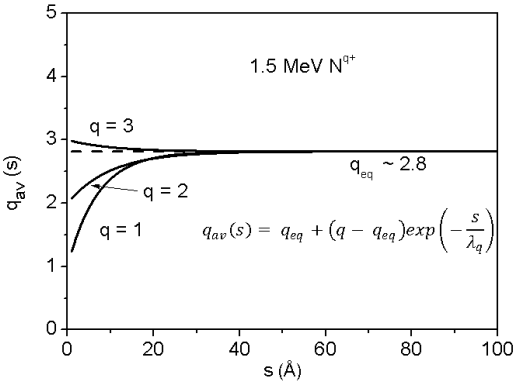

FIG. 6. Average charge state curves in function of the distances reached inside a solid of icy water (λ_q ~ 10 Å) by 1.5 MeV N^{q+} ion beams with initial charges 1 and 3 [22]. For valine, λ_q is not known, but the order of magnitude is expected to be the same.

The disagreement by one order of magnitude presented in Figure 4 (a) reflects that either an experimental difficulty occurs (e.g., the actual beam charge state impinging on the sample is not well known), or sputtering is relevant. In the latter direction, Figure 4 (b) shows the average σ_d^{ap} dependence on q^4. Considering $Y(q) = Y(1)\, q^4$, the surprisingly good linear fitting $\sigma_d^{ap}(q) = \sigma_d^{ap}(0) + (Y(1)/N_0)\, q^4$ provides $\sigma_d^{ap}(0) = 1.5 \times 10^{-13}$ cm^2 and $Y(1)/N_0 = 0.061 \times 10^{-13}$ cm^2. Since the sample thickness $z_{sp} = 25$ nm corresponds to $N_0 = 1.6 \times 10^{16}$ molec cm^{-2}, one gets $Y(1) \sim 100$ molec per impact.

4.2. Sputtering measurement from distinct thick targets

Fig. 3 displays data of valine samples with distinct thicknesses bombarded by 1.5 MeV N^+. Figures 7 (a) – (c) present the normalized column densities for three samples as a function of F/N_0. The green dashed curves are fittings of the average behavior of the considered bands.

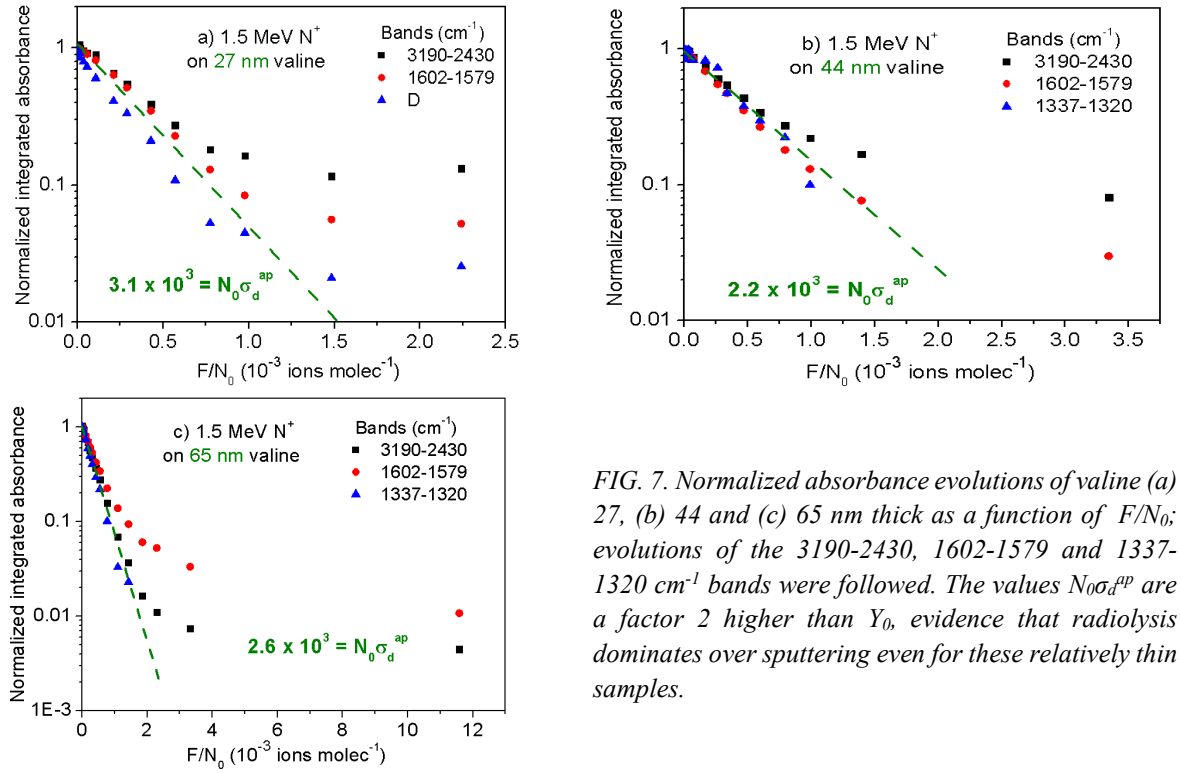

FIG. 7. Normalized absorbance evolutions of valine (a) 27, (b) 44 and (c) 65 nm thick as a function of F/N_0; evolutions of the 3190-2430, 1602-1579 and 1337-1320 cm^{-1} bands were followed. The values $N_0\sigma_d^{ap}$ are a factor 2 higher than Y_0, evidence that radiolysis dominates over sputtering even for these relatively thin samples.

Another analysis of the same fact is exhibited in Fig. 8. The dispersion of the analyzed bands on each measurement is not negligible, see Table 4. Since $\sigma_d^{ap} = \sigma_d + Y_0/N_0$, the average σ_d^{ap} is plotted as a function of the inverse of the corresponding initial column density, in an attempt to measure individually σ_d and Y_0. From Fig. 8, Y_0 is approximately 1300 ± 700 molecules per impact, and $\sigma_d = (7.0 \pm 3) \times 10^{-14}$ cm^2. For thin and thick films, the sputtering yield is 2 to 20 times lower than the rate $N_0\sigma_d^{ap}$. The finding that $Y_0 \sim 10^3$ molecules per impact is to be compared with the sputtering yield for ices, which are two orders of magnitude higher (e.g., Mejía et al. (2020) [28]).

TABLE 4. Apparent destruction cross sections of 27, 44 and 65 nm valine samples.

Thickness (nm)	N_0 (10^{16} cm^{-2})	σ_d^{ap} (10^{-14} cm^2)				$N_0\,\sigma_d^{ap}$
		Analyzed band (cm^{-1})			Average	
		3190-2430	1602-1579	1337-1320		
25	1.6	9.6	9.6	22	14 ± 8	2240
27.5	1.8	14	14	22	17 ± 5	3060
44	3.0	7.1	7.9	-	10 ± 6	2250
65	4.4	5.4	6.2	6.4	6.0 ± 0.6	2640
230	15	7.2	-	7.6	11* ± 4	16x10^3

*Average performed with the σ_d of the bands presented in the table and those of the 1279-1261, 957-937, 782-763, and 726-705 cm^{-1} bands [29].

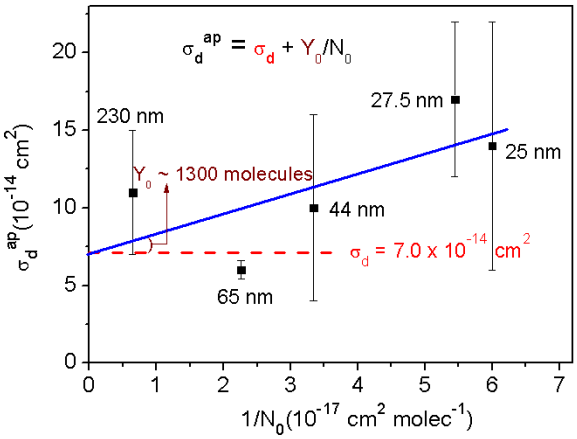

FIG. 8. Average apparent destruction cross section of valine irradiated by 1.5 MeV N^+ in function of the inverse initial column density. $Y_0 \sim 1300 \pm 700$ molecules/projectile and $\sigma_d = (7.0 \pm 3) \times 10^{-14}$ cm^2 are the estimated sputtering yield and destruction cross section, respectively.

5. CONCLUSIONS

Nitrogen MeV ions under distinct conditions (different beam energies and charges) were employed to irradiate valine. FTIR spectroscopy analysis provides the following conclusions:

- Changing projectile species has no effect on the sample chemical modification, with exception of their destruction absolute cross sections that depend on the deposited dose;
- Radiolysis and sputtering are the phenomena responsible for the amino acids degradation - with the main reactions being decarboxylation and deamination [30-32]. Column densities decrease exponentially as a function of beam fluence. FTIR technique is not able to discriminate the effects of the two processes, so that only the sum of them, $\sigma_d^{ap} = \sigma_d + Y_0/N_0$, is determined;
- For MeV ion beams, it turns out that σ_d^{ap} data is compatible with the suggestion that it is proportional to the electronic stopping power and, consequently, to the absorbed dose. Indeed, this relationship holds for glycine and phenylalanine and for similar organic materials such as adenine (e.g., [30, 33]). However $\sigma_d^{ap} = aS_e^n$, with n = 1.0, is not valid for condensed gases, where values lay in-between $1.3 \leq n \leq 1.5$ [34-36];

— For five valine samples with different thicknesses, the sputtering yield, Y_0, for the beam 1.5 MeV N^+ is estimated to be around 1300 ± 700 molecules per impact, while the absolute destruction cross section, σ_d, is predicted to be (7.0 ± 3) x 10^{-14} cm^2 (see Fig. 8);
— Preliminary results with multi-charged beams show that experimental data do not agree qualitatively with σ_d^{ap} predictions based on Joy-Luo or CasP calculations. The finding that $\sigma_d^{ap} \sim q^4$ indicates that for charge states $q > 2$ sputtering damaging effects dominate over the radiolysis ones and yields $Y_0 \sim 100$ precursors per impact for 1.5 MeV N^+ beam. This yield is one order of magnitude lower than the one estimated from varying sample thicknesses;
— If the incident projectile charge is different from the equilibrium charge, multi-charged beam analysis predicts that radiolysis damage rate varies in the bulk along the characteristic relaxation length λ_q. This values, for MeV N^{q+} beams, are in the nanometer range, a distance too short for hadronterapy aplications. Increasing the beam energy into the 100 MeV – 1 GeV range will enlarge λ_q by orders of magnitude, but, unfortunately, it is still too short to compensate the difficulties and costs that a high energy and low charge beam brings.

ACKNOWLEDGEMENTS

This study was financed in part by the Coordenação de Aperfeiçoamento de Pessoal de Nível Superior - Brasil (CAPES) – Finance Code 001. We acknowledge the Brazilian agencies FAPERJ (E-26/201.769/2017, E-26/202.843/2018 and E-26/200.413/2020) and CNPq (PDS n° 118349/2017-1) for partial financial support.

REFERENCES

[1] Cronin, J. R. and Moore, C. B. (1971). Amino Acid Analyses of the Murchison, Murray, and Allende Carbonaceous Chondrites. Science 172 1327–9.
[2] Wolman, Y., Haverland, W. J. and Miller, S. L. (1972). Nonprotein Amino Acids from Spark Discharges and Their Comparison with the Murchison Meteorite Amino Acids. Proceedings of the National Academy of Sciences 69 809–11.
[3] Cronin, J. R. and Moore, C. B. (1976). Amino acids of the Nogoya and Mokoia carbonaceous chondrites. Geochimica et Cosmochimica Acta 40 853–7.
[4] Elsila, J. E., Glavin, D. P. and Dworkin, J. P. (2009). Cometary glycine detected in samples returned by Stardust. Meteoritics & Planetary Science 44 1323–30.
[5] Altwegg, K., Balsiger, H., Bar-Nun, A., Berthelier, J.-J., Bieler, A., Bochsler, P., Briois, C., Calmonte, U., Combi, M. R., Cottin, H., De Keyser, J., Dhooghe, F., Fiethe, B., Fuselier, S. A., Gasc, S., Gombosi, T. I., Hansen, K. C., Haessig, M., Jäckel, A., Kopp, E., Korth, A., Le Roy, L., Mall, U., Marty, B., Mousis, O., Owen, T., Rème, H., Rubin, M., Sémon, T., Tzou, C.-Y., Hunter Waite, J. and Wurz, P. (2016). Prebiotic chemicals—amino acid and phosphorus—in the coma of comet 67P/Churyumov-Gerasimenko. Sci. Adv. 2 e1600285.
[6] Cruz-Diaz, G. A., Erickson, S. E., Silveira, E. F. da, Ricca, A., de Barros, A. L. F., da Costa, C. A. P., Pereira, R. C. and Mattioda, A. L. (2019). PAH Products and Processing by Different Energy Sources. ApJ 882 44.
[7] Iglesias-Groth, S., Cataldo, F., Ursini, O. and Manchado, A. (2010). Amino acids in comets and meteorites: stability under gamma radiation and preservation of the enantiomeric excess: Amino acids in comets and meteorites. Monthly Notices of the Royal Astronomical Society no-no.
[8] Cataldo, F., Angelini, G., Iglesias-Groth, S. and Manchado, A. (2011). Solid state radiolysis of amino acids in an astrochemical perspective. Radiation Physics and Chemistry 80 57–65.
[9] Cataldo, F., Ragni, P., Iglesias-Groth, S. and Manchado, A. (2011). A detailed analysis of the properties of radiolyzed proteinaceous amino acids. J Radioanal Nucl Chem 287 903–11.
[10] Sagan, C. and Khare, B. N. (1979). Tholins: organic chemistry of interstellar grains and gas. Nature 277 102–7.
[11] Strazzulla, G. (1997). Ion irradiation: Its relevance to the evolution of complex organics in the outer solar system. Advances in Space Research 19 1077–84.
[12] Degiovanni A., Amaldi, U. (2015). History of hadron therapy accelerators. Physica Medica, 31 322–332.
[13] Pilling, S., Mendes, L. A. V., Bordalo, V., Guaman, C. F. M., Ponciano, C. R. and da Silveira, E. F. (2013). The Influence of Crystallinity Degree on the Glycine Decomposition Induced by 1 MeV Proton Bombardment in Space Analog Conditions. Astrobiology 13 79–91.

[14] da Costa, C. A. P., Souza-Corrêa, J. A. and da Silveira, E. F. (2021). Infrared analysis of Glycine dissociation by MeV ions and keV electrons. Monthly Notices of the Royal Astronomical Society 502 2105–19.
[15] ANON. (1989). The Merck Index. Merck & Co. Inc.: Rahway, NJ.
[16] Seperuelo Duarte, E., Domaracka, A., Boduch, P., Rothard, H. and Dartois, E. (2010). Laboratory simulation of heavy-ion cosmic-ray interaction with condensed CO.
[17] Wittkower, A. B. (1973). Equilibrium-Charge-State Distributions Of Energetic Ions (Z ~ 2) In Gaseous And Solid Media. 5 54.
[18] Grande, P. L. and Schiwietz, G. (1998). Impact-parameter dependence of the electronic energy loss of fast ions. Phys. Rev. A 58 3796–801.
[19] Bethe, H. A., Ashkin, J. and et al. (1953). Experimental nuclear physic.
[20] Joy, D. C. and Luo, S. (1989). An empirical stopping power relationship for low-energy electrons. Scanning 11 176–80.
[21] Betz, H.-D. (1972). Charge state and charge-changing cross sections of fast heavy ions penetrating through gaseous and solid media.
[22] Toapanta, P. D. I. (2006). Extensão Do Modelo De Traço Nuclear Para Descrever A Dessorção Iônica: Aplicação Aos Agregados De Água. PUC-Rio, Rio de Janeiro.
[23] Niggas, A., Creutzburg, S., Schwestka, J., Wöckinger, B., Gupta, T., Grande, P. L., Eder, D., Marques, J. P., Bayer, B. C., Aumayr, F., Bennett, R. and Wilhelm, R. A. (2021). Peeling graphite layer by layer reveals the charge exchange dynamics of ions inside a solid. Commun Phys 4 180.
[24] Nastasi, M., Michael, N., Mayer, J., Hirvonen, J. K. and James, M. (1996). Ion-solid interactions: fundamentals and applications. Cambridge University Press.
[25] Montenegro, E. C., Cruz, S. A. and Vargas-Aburto, C. (1982). A universal equation for the electronic stopping of ions in solids. Physics Letters A 92 195–202.
[26] Heckman, H. H., Hubbard, E. L. and Simon, W. G. (1963). Electronic Charge Distributions for Heavy Ions at High Velocities. Phys. Rev. 129 1240–9.
[27] Bohr, N. Velocity-Range Relation for Fission Fragments. 6.
[28] Mejía, C., de Barros, A. L. F., Rothard, H., Boduch, P. and da Silveira, E. F. (2020). Radiolysis of Ices by Cosmic-Rays: CH 4 and H 2 O Ices Mixtures Irradiated by 40 MeV 58 Ni 11+ Ions. ApJ 894 132.
[29] da Costa, C. A. P., Muniz, G. S. V., Boduch, P., Rothard, H. and Silveira, E. F. da. (2020). Valine Radiolysis by H+, He+, N+, and S15+ MeV Ions. IJMS 21 1893.
[30] Gerakines, P. A., Hudson, R. L., Moore, M. H. and Bell, J.-L. (2012). In situ measurements of the radiation stability of amino acids at 15–140 K. Icarus 220 647–59.
[31] Meshitsuka, G., Shindo, K., Minegishi, A., Suguro, H. and Shinozaki, Y. (1964). Radiolysis of Solid Glycine. BCSJ 37 928–30.
[32] Gerakines, P. A. and Hudson, R. L. (2013). Glycine's radiolytic destruction in ices: first in situ laboratory measurements for Mars. Astrobiology 647–55.
[33] Vignoli Muniz, G. S., Mejía, C. F., Martinez, R., Auge, B., Rothard, H., Domaracka, A. and Boduch, P. (2017). Radioresistance of Adenine to Cosmic Rays. Astrobiology 17 298–308.
[34] de Barros, A. L. F., Bordalo, V., Seperuelo Duarte, E., F da Silveira, E., Domaracka, A., Rothard, H. and Boduch, P. (2011). Cosmic ray impact on astrophysical ices: laboratory studies on heavy ion irradiation of methane. A&A 531 A160.
[35] Andrade, D. P. P., de Barros, A. L. F., Pilling, S., Domaracka, A., Rothard, H., Boduch, P. and da Silveira, E. F. (2013). Chemical reactions induced in frozen formic acid by heavy ion cosmic rays. Monthly Notices of the Royal Astronomical Society 430 787–96.
[36] Mejía, C. F., de Barros, A. L. F., Bordalo, V., da Silveira, E. F., Boduch, P., Domaracka, A. and Rothard, H. (2013). Cosmic ray–ice interaction studied by radiolysis of 15 K methane ice with MeV O, Fe and Zn ions. Monthly Notices of the Royal Astronomical Society 433 2368–79.